THE JOURNAL OF BIOLOGICAL CHEMISTRY VOL. 287, NO. 12, pp. 8714–8723, March 16, 2012

Identification of Small Molecule Inhibitors of Neurite Loss Induced by Aβ peptide using High Content Screening*[S]

Received for publication, August 9, 2011, and in revised form, January 5, 2012 Published, JBC Papers in Press, January 25, 2012, DOI 10.1074/jbc.M111.290957

Dimitry Ofengeim[‡], Peng Shi[§], Benchun Miao[¶], Jing Fan[§], Xiaofeng Xia[§], Yubo Fan[§], Marta M. Lipinski[‡], Tadafumi Hashimoto[‖], Manuela Polydoro[‖], Junying Yuan[‡], Stephen T. C. Wong[§1], and Alexei Degterev[¶2]

From the [‡]Department of Cell Biology, Harvard Medical School, Boston, Massachusetts 02115, the [§]Department of Systems Medicine and Bioengineering, Methodist Hospital Research Institute, Houston, Texas 77030, the [¶]Department of Biochemistry, Tufts University School of Medicine, Boston, Massachusetts 02111, and the [‖]Department of Neurology/Alzheimer's Disease Research Laboratory, Massachusetts General Hospital, Charlestown, Massachusetts 02129

Background: Amyloid-β-induced degeneration of neurites is a key event in Alzheimer disease.
Results: We describe NeuriteIQ high content screening platform for analysis of neurite degeneration.
Conclusion: We identified multiple cyclooxygenase inhibitors and agonists of PPARγ as suppressors of Aβ-induced neurite loss.
Significance: Our study demonstrates the feasibility of using NeuriteQ to discover inhibitors of neurite loss and provide a new insight into neurite degeneration.

Multiple lines of evidence indicate a strong relationship between Aβ peptide-induced neurite degeneration and the progressive loss of cognitive functions in Alzheimer disease (AD) patients and in AD animal models. This prompted us to develop a high content screening assay (HCS) and Neurite Image Quantitator (NeuriteIQ) software to quantify the loss of neuronal projections induced by Aβ peptide neurons and enable us to identify new classes of neurite-protective small molecules, which may represent new leads for AD drug discovery. We identified thirty-six inhibitors of Aβ-induced neurite loss in the 1,040-compound National Institute of Neurological Disorders and Stroke (NINDS) custom collection of known bioactives and FDA approved drugs. Activity clustering showed that non-steroidal anti-inflammatory drugs (NSAIDs) were significantly enriched among the hits. Notably, NSAIDs have previously attracted significant attention as potential drugs for AD; however their mechanism of action remains controversial. Our data revealed that cyclooxygenase-2 (COX-2) expression was increased following Aβ treatment. Furthermore, multiple distinct classes of COX inhibitors efficiently blocked neurite loss in primary neurons, suggesting that increased COX activity contributes to Aβ peptide-induced neurite loss. Finally, we discovered that the detrimental effect of COX activity on neurite integrity may be mediated through the inhibition of peroxisome proliferator-activated receptor γ (PPARγ) activity. Overall, our work establishes the feasibility of identifying small molecule inhibitors of Aβ-induced neurite loss using the NeuriteIQ pipeline and provides novel insights into the mechanisms of neuroprotection by NSAIDs.

Abnormal processing of Amyloid Precursor Protein, resulting in the formation of amyloid-β (Aβ)[3] peptide oligomers, has emerged as a principle trigger of progressive loss of neuronal function and cell death during Alzheimer disease (1). At the cellular level, this disease is characterized by degeneration of neuronal projections, loss of dendritic spine density and neuronal loss (2). The development of cognitive impairment strongly correlates with the accumulation of soluble Aβ oligomers in AD brains (3). Significant effort has been made to understand the mechanisms of cell death triggered by Aβ. However, there is evidence that cognitive decline correlates better with synaptic changes than with the eventual neuronal death. For example, no significant neuronal death was observed at the onset of cognitive decline in the Tg2576 APPSw mice (4). Furthermore, loss or dystrophy of neurites is a common feature of several neurodegenerative processes such as Parkinson disease, dementia with Lewy bodies and amyotrophic lateral sclerosis (5, 6). Therefore, development of an assay, which would allow identification of new classes of molecules capable of protecting neurites will be very useful for many areas of neurodegeneration. In the present report, we have focused on the development of a NeuriteIQ HCS pipeline and show its use in reliably screening and characterizing small molecules that are protective against Aβ-induced neurite loss. To the best of our knowledge, this is the first use of HCS and analysis to systematically and specifically identify drugs that prevent neurite loss caused by Aβ in primary neurons.

We used the NINDS library of known bioactive compounds for our screen, as the knowledge of targets of many compounds in this library would provide new insights into the mechanisms of regulation of neurite loss. Furthermore, because the library

* This work was supported, in whole or in part, by National Institutes of Health Grants R01AG028928, NIH R01 LM009161, John S Dunn Research Foundation, TT and WF Chao Family Foundation (to S. T. C. W.), and Smith Family Award for Excellence in Biomedical Research (to A. D.).
[S] This article contains supplemental Figs. S1–S4.
[1] To whom correspondence may be addressed: Weill Cornell Medical College of Cornell University.
[2] To whom correspondence may be addressed: Tufts University, 136 Harrison Ave., Boston, MA 02111. E-mail: alexei.degterev@tufts.edu.

[3] The abbreviations used are: Aβ, amyloid-β peptide; APP, amyloid precursor protein, AD, Alzheimer disease; NSAIDs, non-steroidal anti-inflammatory drugs; COX-1/2, cyclooxygenase-1/2; PPARγ, peroxisome proliferator-activated receptor γ; HCS, high content screening; ANL, average neurite length; PPRE, peroxisome proliferator response element; RhoA, Ras homolog gene family member A.

includes FDA-approved drugs, it may reveal promising molecules for expedited development. Our results point to the role of cyclooxygenases in Aβ-induced neurite loss. Cyclooxygenases are enzymes regulating synthesis of prostaglandins. NSAID inhibitors of COX enzymes are widely used as anti-inflammatory drugs. Interestingly, NSAIDs, inhibitors of COX-1 and COX-2, have been widely tested for AD (including multiple clinical trials). The results were inconsistent with both positive effects and no benefits being reported (7) and the mechanisms of NSAIDs' function remain controversial. The rationale for testing NSAIDs in previous studies was to target neuroinflammation, rather than protection against Aβ-induced neurite loss. Our data reveal neurite protection as a general mechanism of activity of NSAIDs, which should be considered in future re-evaluation of the potential of this important class of drugs as treatments for AD.

MATERIALS AND METHODS

Cortical Neuron Culture—Neurons were obtained as described (8). Briefly, C57BL/6 mouse embryo (E15) brains were dissected and trypsinized at room temperature (RT), followed by trituration. Neurons were resuspended in DMEM medium supplemented with 10% FBS, 100 units/ml penicillin, 100 μg/ml streptomycin, and 2 mM glutamine, and seeded in 384-well plates at 1×10^4 cells/well. The following day medium was changed to neurobasal with B27, penicillin/streptomycin, and glutamine and incubated for 4 days. Following treatment, neurons were incubated (37 °C) for 3 days before fixation and staining.

Aβ Preparation and Characterization—Aβ_{1-40} and Aβ_{1-42} were dissolved in water at 400 μM and pre-formed fibrils were separated by centrifugation for 1 h at 100,000 $\times$ *g*. Soluble fractions were diluted in 0.1 M Tris-HCl buffer (pH 7.4) to 200 μM, incubated for 1–4 h (37 °C) and added to the cells after dilution with neurobasal media to a final concentration of 5 μM.

For the analysis of Aβ oligomers, the aliquots of peptides were immediately put on ice following aggregation, and 3 mM thioflavin T in 0.1 M glycine-NaOH (pH 8.5) buffer prechilled at 4 °C was added. Fluorescence of the samples was determined using fluorescence spectrophotometer F2500 (Hitachi) at λ_{ex} of 443 nm and λ_{em} of 484 nm. Fluorescence of 500 μl aliquot of 3 mM thioflavin T solution was subtracted as a blank. Average levels of fluorescence in three independent experiments were analyzed. Following the ThT assay, the oligomeric species were separated by size exclusion chromatography on a Superdex 200 column (GE Healthcare) in 50 mM ammonium acetate pH 8.5 buffer using AKTA purifier 10 (GE Healthcare). Fractions from the column were analyzed by Western blot using the 6E10 antibody (Covance). The results are shown in supplemental Fig. S1.

Neuronal Staining—Neurons were fixed with 4% paraformaldehyde for 30 min (room temperature). Cells were permeabilized with 10% normal donkey serum and 0.4% Triton X-100 for 30 min (room temperature). Primary TUJ1 antibody, and secondary donkey anti-mouse Cy3-conjugated antibody were used to stain neurons; nuclei were stained with Sytox Green. Neurons were imaged on automated CellWorx microscope (Applied Precision) at 10× magnification and 488 nm (Sytox Green) and 550 nm (Cy3) wavelengths.

Image Acquisition and Quantification—We developed the NeuriteIQ software to obtain accurate quantification of neurite lengths in high density neuronal cultures. The software provides an automated pipeline for quantitative interpretation of automatic fluorescence microscopy images, in particular, for the labeling and measurement of neurites. The details of the algorithm are described in detail in Ref. 9, and steps in analysis are shown in Fig. 1*C*. Briefly, to obtain statistical quantifications from neuronal images, NeuriteIQ processes images from Nuclei and Neurite channels separately. In the nuclei channel, total cell number is calculated by image segmentation with local maximum points detection, which separates all the cells from the background, and separates clumped cells from each other based on a watershed method. By comparing with the soma areas detected from corresponding neuron specific image, selection of neurons from non-neuronal cells in the image is performed, providing an accurate neuronal cell number in the whole well.

In the neuron/neurite channel, NeuriteIQ detects soma areas with clustering pixels and higher intensity than adjacent areas. Neurites are then treated as two-dimensional curvilinear structures, which could be detected based on the local Hessian matrix. The Hessian matrix describes the local curvature of a curvilinear structure, which is an useful algorithm that allows detection the center points and local directions of neurite in a field. Subsequently, a specific neurite is detected from a seed point, which is defined as an initial point on or near the center line of a dendritic segment and soma. Therefore, a specific dendrite could be ascribed to a specific nucleus by its seed point. Identification of seed points for each neurite minimizes interference from positively stained debris.

The tracking algorithm then detects center points along each neurite, and defines the possible direction of neurites from each center point. After calculating the center points and their directions, centerlines could be extracted along neurites by linking detected center points along the local directions, which display curvilinear structures. In case of breaks between near branching structures, a predefined radius r is set up to determine whether two end points of different centerlines should be linked together. If one of the end points is in the local direction of another centerline, and the distance between two end points is in the range of r, those two points are linked to fill the break. Bresenham line drawing algorithm is applied to link these two points. This allows us to solve the neurite line break problem during the post-processing of images.

NeuriteIQ provides a statistical quantification of the total neurite length in one image, which is subsequently used to calculate Average Neurite Length (ANL) as the statistical feature of neurite outgrowth in each well. ANL is defined as a ratio between Total Neurite Length per image and Neuron Cell Numbers. ANL is a statistical parameter, which averages the neurite lengths in the entire neuronal field and makes the analysis results resistant to slight changes in the neuron culture and staining as well as local variations in cell density and errors in tracing of individual neurites due to high cell density. ANL calculations are described in detail in Ref. 10. Because both of the total neurite length and neuron cell number are statistical results averaged over entire image, ANL is a robust measure of

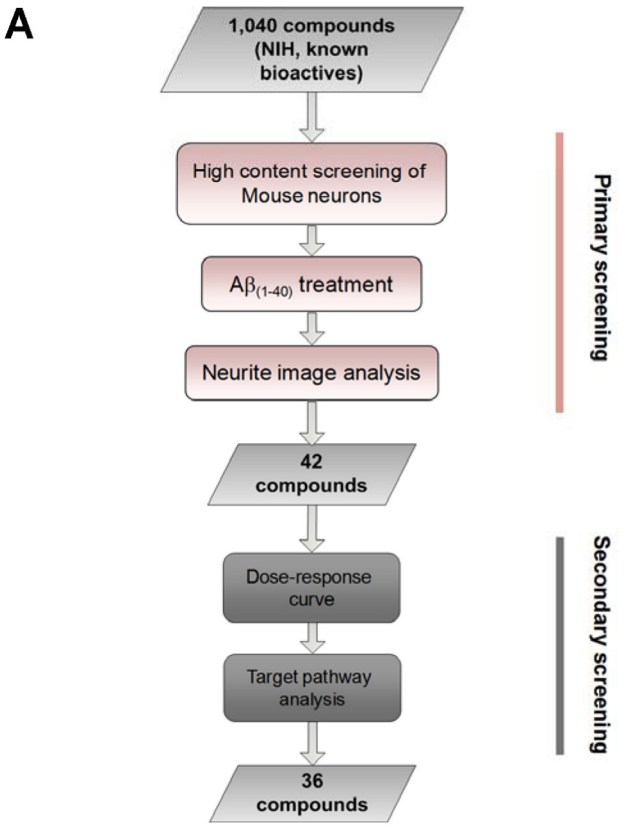
A
1,040 compounds (NIH, known bioactives)
High content screening of Mouse neurons
Aβ(1-40) treatment
Neurite image analysis
42 compounds
Dose-response curve
Target pathway analysis
36 compounds
Primary screening
Secondary screening

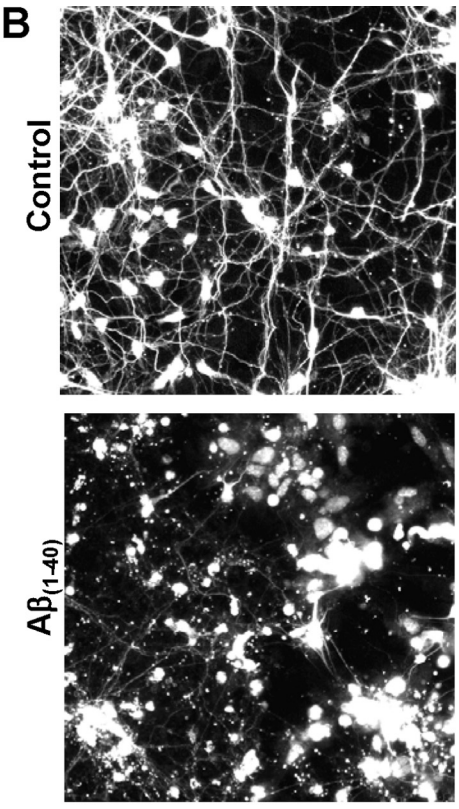
B
Control
Aβ(1-40)

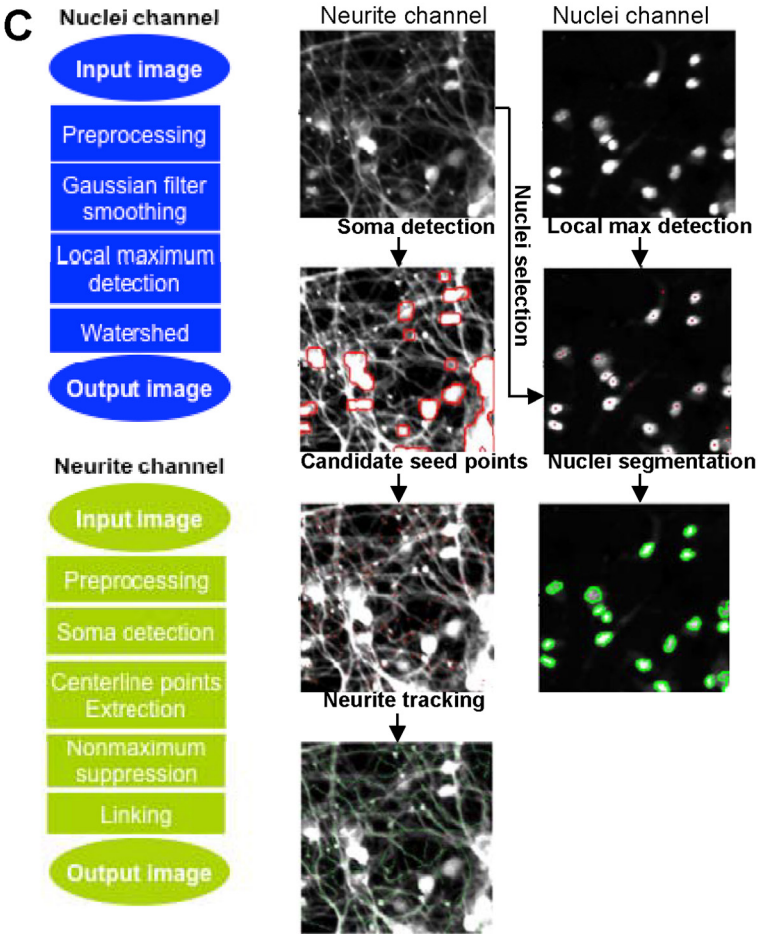
C
Nuclei channel
Input image
Preprocessing
Gaussian filter smoothing
Local maximum detection
Watershed
Output image
Neurite channel
Input image
Preprocessing
Soma detection
Centerline points Extraction
Nonmaximum suppression
Linking
Output image
Neurite channel
Nuclei channel
Soma detection
Local max detection
Nuclei selection
Candidate seed points
Nuclei segmentation
Neurite tracking

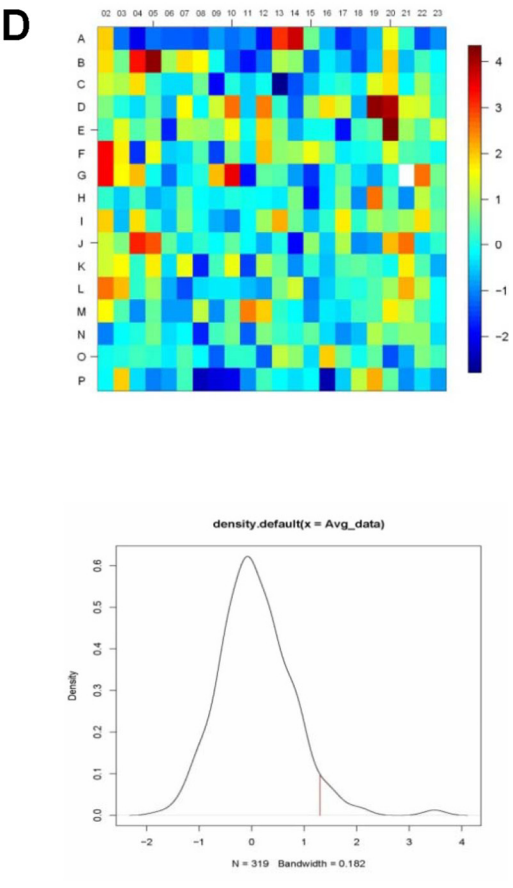
D
density.default(x = Avg_data)
Density
N = 319 Bandwidth = 0.182

neurite outgrowth which is highly accurate and reproducible even in high density cultures. Thus, NeuriteIQ is a fully automated tool for batch processing a large dataset of images without human intervention such as selecting start points of neurites, defining directions for neurite tracking in a branch, etc, which makes NeuriteIQ an efficient tool in dealing with large scale dataset for compound screening. We have made NeuriteIQ public, and it can be downloaded for free along with user documentation on the web. Finally, Z′-factors of ANL (average neurite length) and ANB (average neurite brightness, which is defined as the ratio between the total brightness (intensity) of all neurite pixels and the total length of all neurites in the image,) were calculated to pilot for quality assessment of assay conditions. Despite relatively poor z′ (−0.84 for ANL where $z' = 1 - (3 \times SD_{untreated} + 3 \times SD_{A\beta})/(Average_{untreated} - Average_{A\beta})$) due to the variance typical for primary neurons treated with $A\beta_{1-40}$, this method consistently yielded significant ($p \leq 0.05$) differences between $A\beta_{1-40}$ treated and untreated control groups.

Screen Design—NINDS custom collection compound library II containing 1,040 known bioactive small molecule compounds was used in the primary screen. The details of this library can be viewed on the ICCB-Longwood, the Harvard Medical School webpage. The compounds were robotically added to neurons at a concentration of 25 μM with all compound plates screened in triplicate. Each plate included untreated and $A\beta_{1-40}$-treated control wells. Only plates with significant difference (at least $p \leq 0.1$, usually $p \leq 0.05$ using 2-tailed Student's *t* test) between control groups were used for hit selection. z-scores were calculated based on degree of protection as compared with $A\beta_{1-40}$ treated control where $z = (\text{compound well score} - Average_{A\beta\ control})/SD_{A\beta\ control}$). The following criteria were used for hit selection: 1) average and median z for each hit compound ≥1.5 ($p \leq 0.05$), 2) average z for each hit ≥ z-score difference between untreated and $A\beta_{1-40}$ controls for that specific plate, and 3) visual inspection of hit compound wells confirmed high image quality. This resulted in a total of 42 primary hits (4%). These were re-examined in a secondary screen, under the same conditions, except the compounds were used at 5 concentrations (2.5 nM, 25 nM, 250 nM, and 2.5 μM) to generate an estimated EC_{50} as described below.

Bioinformatics Analysis—Multiple resources (NCBI, Wishart) were used to get drug target information for the analysis. To assess the enrichment of hit compound categories relative to their representation in the NINDS library, *p* values were computed using hypergeometric probability distribution. Categories with $p < 0.05$ were considered enriched. This analysis allowed us to identify functional categories of inhibitors enriched in screening hits and to evaluate the putative roles of these classes of inhibitors in AD.

EC_{50} Calculation—For EC_{50} calculations, neurons were treated with Aβ as above in the presence of either 4 (2.5 nM, 25 nM, 250 nM, and 2.5 μM) or 9 (0.1 nM, 1.0 nM, 10 nM, 50 nM, 100 nM, 500 nM, 1.0 μM, 5 μM, 50 μM, and 100 μM) concentrations compound as described in the text. EC_{50} values were calculated by non-linear regression using GraphPad Prism software. For "EC_{50} (μm) (from 0 to 100%)" column, values represent the concentrations of compound that provide 50% neurite protection relative to the untreated control, which was set as 100%. In "EC_{50} (μm) (from min to max)" column values represent concentrations of compounds providing half protection between the lowest and highest points of each compound curve. N/A indicates lack of fit.

Compounds and Western Blot Analysis—Drugs for secondary screening, NSAID specific compounds and PPARγ targeting compounds were purchased form Cayman Chemical or Sigma. After treatment, cells were harvested and lysed in RIPA buffer (50 mM Tris·HCl at pH 7.5, 150 mM NaCl, 5 mM EDTA, 0.1% SDS, 0.5% sodium deoxycholate, and 1% Nonidet P-40, supplemented with Complete Mini protease inhibitors) and equal amounts of protein were subjected to Western blot analysis using COX2, PPARγ (Santa Cruz Biotechnology), and tubulin (Sigma) antibodies.

PPARγ Transcription Factor Assay Kit—The binding assay was performed according to the manufacturers instructions (Cayman Chemical). Briefly, a specific double-stranded DNA sequence containing the peroxisome proliferator response element (PPRE) is immobilized onto a 96-well plate. PPARs contained in a neuronal nuclear extract were bound to the PPRE and PPARγ was selectively detected using a specific antibody. A secondary antibody conjugated to HRP was added to provide a colorimetric readout at 450 nm. Absorbance values were determined using Victor Wallac3 platereader (Perkin Elmer). Concentrations of nuclear extracts were determined using the Bradford assay (Bio-Rad). Absorbance values were normalized to nuclear extract concentrations and presented as percentages of the untreated control cells. Experiments were performed in triplicate.

RESULTS

High Content Screen for Compounds Suppressing $A\beta_{1-40}$-induced Neurite Degeneration—To identify small molecules that can suppress $A\beta_{1-40}$ induced degeneration of neuronal processes, we screened the 1,040 compound known bioactives NINDS custom collection library II, in primary mouse cortical neurons in the presence of oligomeric $A\beta_{1-40}$ (5 μM). Neurite lengths were quantified using the NeuriteIQ software (Fig. 1*A*, see "Materials and Methods" for the detailed description), in which individual neurons were identified and the average neurite length was determined (Fig. 1*B*). The NeuriteIQ algorithm can accurately calculate a reduction of neurite length in

FIGURE 1. **Analysis of neurite lengths using NeuriteIQ algorithm.** *A*, overview of the screening process used to determine compounds that significantly inhibit $A\beta_{(1-40)}$ neurite loss, as is shown in a representative image in *B*. *C*, flowchart of nuclei detection and segmentation method. In the neurite channel, we extracted the centerline of neurites and their branches simultaneously. The purpose was to evaluate the total average length and intensity of the neurites per neuronal cell. The images to the *right* are a schematic representation of the image processing that NeuriteIQ performs *D*. The heat map shows the z-scores of the 384 well plate calculated based on triplicate experiments, where the z-scores were calculated based on average neurite lengths (*ANL*) as described in the *Screen Design* section of "Materials and Methods." *Dark red* and *dark blue* represent highest and lowest numbers, respectively. Distribution of z-scores is also shown. The hit selection criteria are described in "Materials and Methods."

A

Compound	Category	Z-score	EC_{50} (0-100%)	EC_{50} (min to max)
*mitomycin c	DNA crosslinker/ Alkylating agent	5.458903	N/A	N/A
cyclophosphamide hydrate	Alkylating Agent	5.279908	8.0342	0.769
*gambogic acid	DNA damage inducer	5.032413	N/A	N/A
thiotepa	Alkylating agent	3.643398	5.4694	2.0368
busulfan	Alkylating agent	3.349394	21.4259	8.8928
nimustine	Alkylating agent	2.151972	N/A	N/A
irinotecan hydrochloride	DNA topoisomerase inhibitor	2.132562	0.3531	1.0255
*pyrromycin	DNA damage inducer	6.450958	N/A	N/A
metacetamol	Anti-inflammatory	9.842569	3.6723	6.1227
meloxicam	Anti-inflammatory	4.716366	0.8471	0.4425
naproxol	Anti-inflammatory	3.700361	1.3426	0.769
nabumetone	Anti-inflammatory	3.180137	0.2805	0.2594
aspirin	Anti-inflammatory	2.367709	1.7699	1.6555
ibuprofen	Anti-inflammatory	2.308481	0.1197	0.8769
beta-escin	Anti-histamine	4.5175	N/A	0.6545
azaperone	Anti-histamine	4.24426	0.2032	N/A
antazoline phosphate	Anti-histamine	3.715077	3.8454	1.2617
1r-camphor	anti-histamine	2.118658	0.1652	N/A
trazodone hydrochloride	Anti-histamine	1.612338	1.4059	1.3
erythromycin stearate	Antibiotic	8.994849	6.5757	3.8436
vancomycin hydrochloride	Antibiotic	2.934997	23.8748	N/A
trimethoprim	Antibiotic	2.533161	N/A	N/A
sulfadiazine	Antibiotic	2.481444	25	4.5555
cefoxitin sodium	Antibiotic	2.175836	N/A	N/A
amprolium	Antibiotic	1.686466	1.8111	0.8549
*puromycin hydrochloride	Antibiotic	3.614473	N/A	N/A
nystatin	Antifungal drug	7.005361	12.3293	1.1427
*sulconazole nitrate	Antifungal drug	6.712039	N/A	0.1552
*phenylmercuric acetate	Antifungal drug	4.122238	N/A	N/A
procaine hydrochloride	Anesthetic	12.13419	7.0948	N/A
lidocaine	Anesthetic	2.385437	N/A	0.358
hexylresorcinol	Anesthetic	2.19733	7.2768	0.1592
enalapril maleate	ACE inhibitor	6.222741	N/A	N/A
choline chloride	Cholinergic modulater	3.714614	2.57	5.1492
triamcinolone diacetate	corticosteroid	2.222652	N/A	N/A
tanshinone iia sulfonate sodium	Steroid-like	7.656802	N/A	0.2466
saccharin	Sweetener	7.884879	N/A	1.7456
lithocholic acid	Detergent	6.167945	9.9527	N/A
hydroflumethiazide	Diuretic	4.633811	2.7857	N/A
amethopterin (r,s)	Antifolate drug	2.879726	N/A	N/A
perillic acid (-)	Isoprenylation inhibitor	2.247	N/A	N/A
carbimazole	Thyroid peroxidase inhibitor	2.011414	5.3081	N/A

B

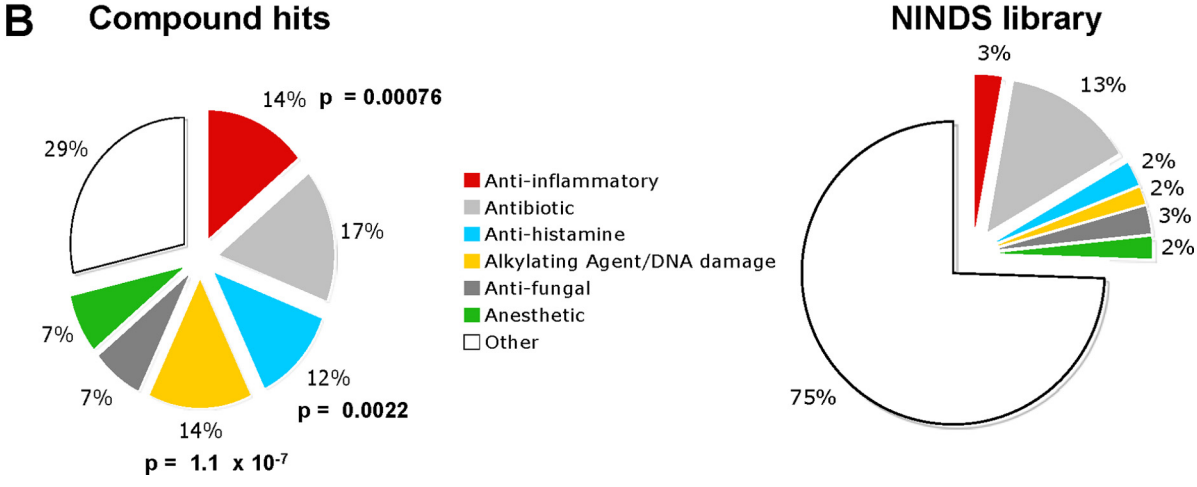

response to $A\beta_{1-40}$ peptide treatment (8) (Fig. 1*C*). To minimize false positives, hits were selected using a high threshold ($\times + 1.5$ S.D.) over ANL values for Aβ-treated control wells in each plate (Fig. 1*D*). In our primary screen, 42 compounds (~0.4%) were identified based on significant ($p \leq 0.05$) protection against $A\beta_{1-40}$-induced neurite loss (Fig. 2*A*). To confirm the specificity of the hits, the compounds were re-examined in a secondary screen and the half maximal effective concentrations (EC_{50}) were estimated. The secondary screen confirmed 36 (85%) compounds (Fig. 2*A* and supplemental Fig. S2) that significantly ($z \geq 2.15$, $p \leq 0.01$) protected primary cortical neurons from $A\beta_{1-40}$ induced-neurite degeneration at micromolar or lower concentrations. Functional clustering of the compound hits identified several drug categories that were enriched when compared with their representation in the NINDS library (Fig. 2*B*). Notably, NSAIDs, anti-histamines and alkylating/DNA-damaging agents were highly enriched among the hits. We believe compounds that showed statistical significance in both the primary and secondary screens are real hits, however, because the drug category did not show significant enrichment as compared with their representation in the library we did not focus on these classes of inhibitors in molecules. These molecules have a broad spectrum of targets, and these will need to be further examined in the future work. These results were promising since all three categories of molecules have been previously investigated as anti-Aβ drugs.

COX Inhibition Blocks Neurite Loss in a Dose-dependent Manner—The NSAID category was of particular interest because several of our hits have received controversial attention as potential Alzheimer therapeutics including naproxol, aspirin, and ibuprofen (11). In addition, metacetamol, meloxicam, and nabumetone were among the validated hits in our screen with their activity confirmed in secondary assay (Figs. 2*A* and 3*A*). While particular NSAIDs might have targets other than cyclooxygenases (COX), the abundance of NSAID hits suggests that COX-1/2 activity may mediate $A\beta_{1-40}$ induced neurite loss. To explore this question, we titrated both ibuprofen and nabumetone in the $A\beta_{1-40}$ induced-neurite loss assay. Ibuprofen and nabumetone protected neurite loss with EC_{50} values of 0.035 and 0.147 μM, respectively (Fig. 3*B*).

The NSAID compounds identified in the screen are capable of inhibiting both COX-1 and COX-2 according to their published activities against recombinant and cellular COX proteins. Thus, to confirm the role of COX enzymes and determine if one of the isoenzymes is necessary for the protective effects of the identified NSAIDs, we utilized a battery of additional COX-1/2 inhibitors (12). Notably, multiple additional inhibitors displayed some degree of neurite protection (Fig. 3, *C* and *D*). Furthermore, both COX-1 and COX-2-specific inhibitors worked in our $A\beta_{1-40}$ assay system. Taken together these results suggest that both COX-1 and COX-2 are needed for Aβ-induced neurite loss.

Finally, we tested several of the hits in the absence of the Aβ peptide, including ibuprofen and meloxicam, and found no effect on neurite lengths at concentrations, which provide protection from Aβ (Fig. 3*E* and supplemental Fig. S3). Therefore, these molecules may specifically interfere with Aβ peptide-induced neurite loss, rather than promoting neurite outgrowth.

While $A\beta_{1-40}$ is the present in the brain at much higher levels (13), $A\beta_{1-42}$ may be a more toxic APP derived peptide. We therefore tested the ability of several NSAIDs to inhibit $A\beta_{1-42}$ dependent neurite loss. Similarly to the shorter $A\beta_{1-40}$, two concentrations of $A\beta_{1-42}$ elicited a significant loss of neurites which was markedly attenuated by ibuprofen, naproxen, and nabumetone (supplemental Fig. S4).

NSAIDs Inhibit Aβ-induced Neurite Loss in a PPARγ-dependent Manner—Recent evidence suggests that ibuprofen can promote neurite growth through a PPARγ-mediated pathway (14). NSAIDs elicited neurite outgrowth at high concentrations (*e.g.* >100 μM ibuprofen, Fig. 3*E*), while our data points to Aβ-specific activity of multiple NSAIDs at low micromolar concentrations. However, a reported connection between ibuprofen and PPARγ prompted us to further examine the possible role of PPARγ in the Aβ-specific activity of NSAIDs. Indeed, Aβ-induced neurite loss was completely reversed in the presence of the selective PPARγ agonist 5-deoxy-Δ12,14-prostaglandin J2 (10 μM) suggesting that PPARγ activity alone is sufficient to rescue neurite loss. Furthermore, while 10 μM ibuprofen effectively inhibited Aβ-induced neurite loss, this effect was eliminated in the presence of PPARγ antagonist, GW 9662 (1 μM, Fig. 4*A*). As PPARγ is a transcription factor, we next investigated the possibility that Aβ treatment inhibits its nuclear activity. Aβ caused a marked reduction of PPARγ DNA binding activity (Fig. 4*B*). Furthermore, not only ibuprofen, as previously reported (14), but also nabumetone and naproxen rescued PPARγ activity in Aβ-treated samples (Fig. 4*B*) at concentrations that prevent Aβ-induced neurite loss. NSAIDs predominantly affected PPARγ DNA binding in Aβ-treated neurons, but had minimal effect on control cells, consistent with the specific roles of COX and PPARγ in Aβ-induced signaling leading to neurite loss. In addition, we determined that COX-2 protein levels were increased in Aβ-treated neurons (Fig. 4, *C* and *D*); ibuprofen did not attenuate Aβ-induced COX-2 increase. The increase in COX-2 protein levels following Aβ treatment did not alter PPARγ protein expression. Taken together these data suggest a model in which COX activity and/or expression is elevated in neurons following Aβ treatment leading to inhibition of PPARγ signaling and contributing to neurite loss. Thus, NSAIDs reduce COX activity and promote PPARγ-dependent neurite protection/recovery.

DISCUSSION

The loss of synaptic connections and neuronal projections is a common feature in neurodegenerative diseases such as Par-

FIGURE 2. **Inhibitors of Aβ-induced neurite loss identified in NeuriteIQ high content screen.** *A*, compounds that protect against $A\beta_{(1-40)}$-induced neurite loss. Forty-two compounds were identified in a primary screen and clustered based on their functional categories. Following the secondary screen, six compounds did not fulfill the criteria (indicated with *). EC_{50} values were estimated using 2.5 nM, 25 nM, 250 nM, and 2.5 μM of the compounds as described under "Materials and Methods." *N/A*, the inhibition curves could not be fit using non-linear regression. *B*, hits were clustered based on their targets or mechanism of action; the enrichment of certain categories is shown as compared with their representation in the NINDS library. The *p* values based on hypergeometric distributions are indicated next to each category for which significant enrichment was identified.

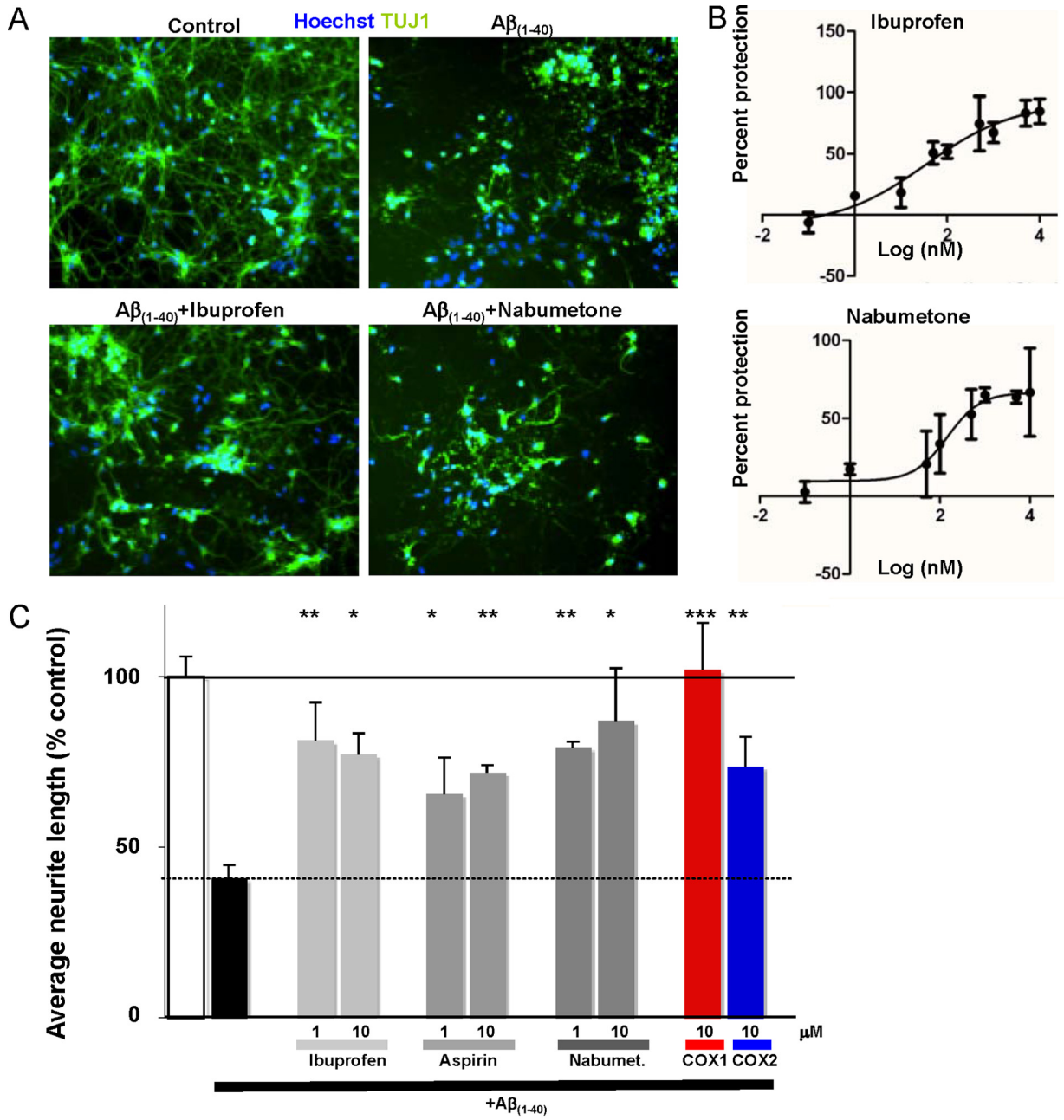
A
Control
Hoechst TUJ1
Aβ(1-40)
Aβ(1-40)+Ibuprofen
Aβ(1-40)+Nabumetone
B
Ibuprofen
Percent protection
Log (nM)
Nabumetone
Percent protection
Log (nM)
C
Average neurite length (% control)
1 10 1 10 1 10 10 10 μM
Ibuprofen
Aspirin
Nabumet.
COX1 COX2
+Aβ(1-40)
D
Average neurite length (% control)
Aβ(1-40)
Indom.Flurb.FR122
SC581Melox.CAY
COX-1 > COX-2
COX-2 > COX-1
E
Average neurite length (μm)
10 nM 1 μM 100 μM
10 nM 1 μM 100 μM
CTL
Ibuprofen
Meloxicam

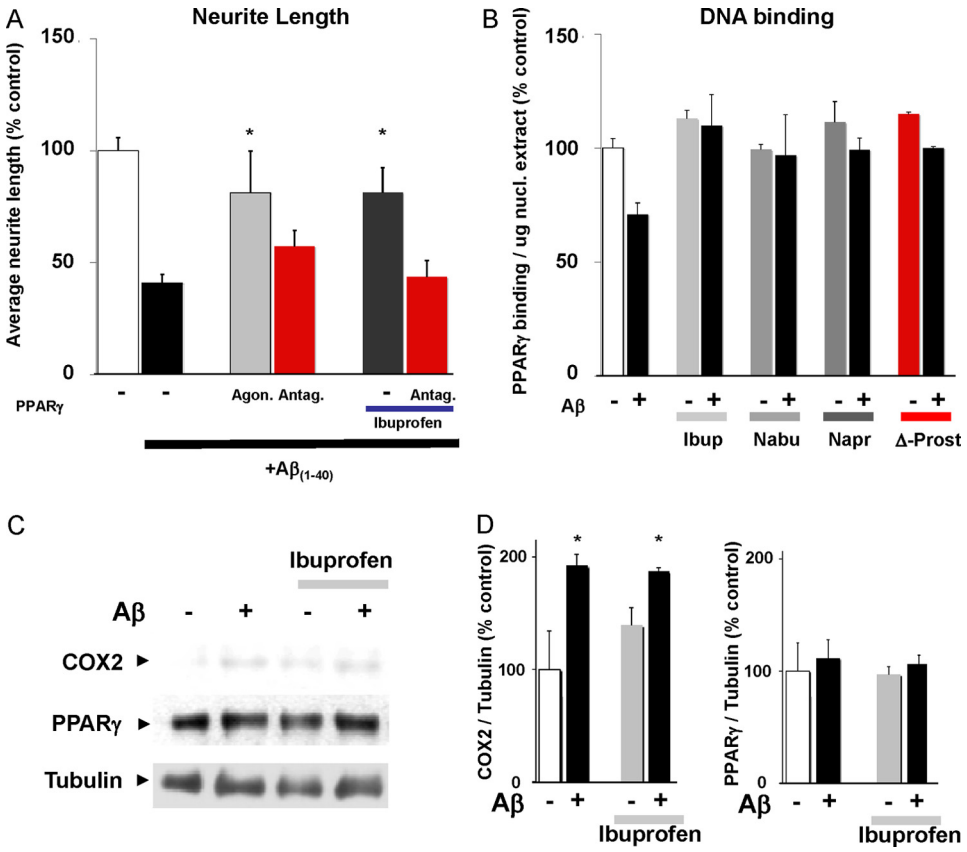

FIGURE 4. **A$\beta_{(1-40)}$-induced neurite loss is mediated by inhibition of PPARγ signaling.** *A*, A$\beta_{(1-40)}$-induced neurite loss is attenuated by PPARγ agonist, 5-deoxy-Δ12,14-prostaglandin J2 (10 μM). Furthermore, neurite protection mediated by ibuprofen is inhibited by the PPARγ antagonist, GW 9662 (1 μM). *B*, A$\beta_{(1-40)}$ elicits a decrease in PPARγ binding to DNA. Ibuprofen facilitates PPAR activity, and preserves PPARγ activity even in the presence of A$\beta_{(1-40)}$. Similarly, nabumetone and naproxen (10 μM) maintain PPARγ after A$\beta_{(1-40)}$ treatment. In contrast, PPARγ agonist, 5-deoxy-Δ12,14-prostaglandin J2, increases PPARγ activity both in control and A$\beta_{(1-40)}$ treatment, as expected. *C*, Western blot showing that A$\beta_{(1-40)}$ promotes an increase in COX2 protein levels, which is unaffected by treatment with ibuprofen; no change in total PPARγ protein levels is observed under any condition. Levels of COX2 and PPARγ expression, normalized to tubulin, are quantified in *D*.

kinson and Alzheimer. Neurite degeneration precedes cell death, suggesting that neurite loss might be a primary cause of cognitive function decline (15). Recent reclassification of AD suggests that pathophysiology begins many years before the diagnosis of AD dementia (16). Therefore, chemical compounds attenuating neurite loss or promoting neurite outgrowth could represent promising new treatments in AD.

HCS using primary neurons is hampered by intrinsic difficulties, such as variability in cell density throughout the well and well-to-well, the need to distinguish between the neuronal and non-neuronal cells present in the cultures, the need for extended culturing of neurons for neurite development, and difficulties in accurately quantifying neurite lengths in complex dense neuronal cultures. The NeuriteIQ pipeline introduces a number of elements to address these difficulties, such as: (*a*) imaging large well areas at 10× magnification to reduce the effects of differences in intrawell densities, (*b*) use of neuron-specific neurite labeling, (*c*) nuclear staining, which provides means to normalize neurite lengths to cell numbers and to exclude positively labeled debris not connected to nuclei, and (*d*) filtering nuclei not connected to neurites, which eliminates non-neuronal cells. These NeuriteIQ features in conjunction with statistical analysis of hits relative to the positive and negative controls in each plate and screening the library in triplicate resulted in a highly reliable hit selection. 36 of 42 screening hits displayed activity in our secondary assay. Overall, these data suggest that the NeuriteIQ screening procedure provides a reliable tool for discovery of novel neurite-protective molecules and putative AD drug candidates. Furthermore, NeuriteIQ can be easily extended to other applications in neurodegeneration.

Our screen of 1,040 compounds from the NINDS collection of known bioactives and FDA approved drugs identified several functional categories of inhibitors, including NSAIDs, anti-histamine drugs, antibiotics, DNA-damaging agents, and regula-

FIGURE 3. **Inhibition of Aβ-induced neurite loss by NSAIDs.** *A*, representative images stained with nuclei labeled with Sytox green in *blue* and neuronal-specific tubulin (*TUJ1*) in *green*. The *upper right panel* shows a reduction in neurite length following A$\beta_{(1-40)}$-induced neurite loss. *B*, ibuprofen and nabumetone inhibit A$\beta_{(1-40)}$-induced neurite loss in a dose-dependent manner. Activity was determined using 9 concentrations of each molecule (0.1 nM, 1.0 nM, 10 nM, 50 nM, 100 nM, 500 nM, 1.0 μM, 5 μM, 50 μM, and 100 μM). *C*, ibuprofen, aspirin, and nabumetone protect against neurite loss following A$\beta_{(1-40)}$ treatment, furthermore, COX1 (FR122047) and COX2 (CAY10404) specific inhibitors both rescue A$\beta_{(1-40)}$-induced neurite loss. *D*, additional COX1 inhibitors, indomethacin, flurbiprofen, and FR122047 (1 μM), as well as, COX2 inhibitors SC-58125, meloxicam, and CAY10404 (all at 1 μM, except meloxicam at 100 nM), protect A$\beta_{(1-40)}$-induced neurite loss. *E*, low doses of ibuprofen and meloxicam do not change the average neurite length under basal conditions while 100 μM ibuprofen and meloxicam increase the average neurite length.

tors of cholinergic system and protein synthesis machinery. Importantly, a number of identified molecules have known connections to Aβ neurotoxicity. For example, previous work showed that cyclophosphamide, a DNA cross-linking agent and a hit in our screen, decreased tau phosphorylation at Ser-396/404 site (17). This result is consistent with the notion that aberrant neuronal cell cycle re-entry may lead to tau hyperphosphorylation, and thus inhibiting cell cycle progression may be one target of therapeutic intervention. Anti-histamines also showed promise in preclinical trials for the treatment of human cognitive disorders (18). The discovery of six NSAIDs as suppressors of neurite loss was particularly intriguing, since this class of molecules has attracted significant attention as potential AD drugs. While clinical data has been generated, the results were generally not conclusive. Some studies showed benefits of certain NSAIDs in the improvement of cognitive functions or delaying onset of AD. However, other studies showed no improvement (19). Intriguingly, while neuroinflammation, which accompanies development of AD, has been the primary reason for testing NSAIDs, several studies have suggested that the positive effects of this class of drugs are not related to inflammation (or Aβ processing, see below) (20, 21). Multiple additional mechanisms of neuroprotection for NSAIDs have been proposed. These include inhibition of γ-secretase activity, Aβ secretion, and Aβ aggregation (especially by ibuprofen (22)) as well as stimulation of neurite outgrowth by some NSAIDs (ibuprofen and indomethacin), but not by naproxen (14, 23). It is unclear which of these mechanisms reflect the activity of COX enzymes as opposed to other targets of particular structural classes of NSAIDs (24). Importantly, our data show for the first time that a wide range of NSAIDs can attenuate Aβ-induced neurite loss in the presence of processed exogenous Aβ and thus strongly indicate that: 1) NSAIDs target COX proteins to modify cellular signaling responses to Aβ, and 2) NSAIDs target Aβ signaling, rather than Aβ generation/processing to attenuate neurite loss.

Furthermore, while our NSAIDs-PPARγ data are reminiscent of reports showing the role of ibuprofen-dependent regulation of PPARγ/RhoA axis in the regulation of neurite outgrowth, there are critical differences. First, while we observed increased neurite density in control neurons treated with 100 μM ibuprofen (Fig. 3*E*), consistent with published data (14), inhibition of Aβ-mediated neurite loss was observed at much lower concentrations, consistent with distinct mechanisms of the two effects. Second, our data show that direct neurite protection is a general property displayed by a wide range of NSAIDs, while previous studies suggested that stimulation of neurite outgrowth is a property of only a subset NSAIDs. Overall, these data along with the observed increase in COX-2 expression in Aβ-treated cells are consistent with the specific roles of COX proteins and PPARγ in Aβ signaling, which represents an important new direction for investigation. This conclusion may explain published *in vivo* observations, such as reports of an improvement in the cognitive function exerted by different COX inhibitors in Tg2576 transgenic AD mouse model, which did not correlate either with inhibition of neuroinflammation or lowering of Aβ levels in the brain (20). Further analysis of the effects of NSAIDs as well as changes in COX and PPARγ activity *in vivo*, especially in regards to changes in neurite architecture, will be important to explain and expand on the promising results reported using NSAIDs for the treatment of AD.

Based on our data we believe that NSAIDs may represent a therapeutically viable option to prevent or delay Alzheimer at the earliest stages of the disease. This is consistent with many epidemiological reports that positive effects of NSAIDS when used on for long-term treatment (US Veterans Affairs Health Care System Study (25), Cache County Study (26), Cardiovascular Health Cognition Study (27), Chicago Health and Aging Project (28)). It is also quite interesting to note that in several clinical trials involving patients who already display mild to moderate cognitive decline (Alzheimer Disease Cooperative Study (ADCS) group (29)) NSAIDs showed no benefit. On the other hand, PPARγ agonist has shown some effectiveness at this stage of the disease (30). Overall, our data present an intriguing possibility that NSAIDs should be specifically re-evaluated as the earliest treatment of Alzheimer, when the disease manifests at the subclinical levels, and, as it progresses, PPARγ agonists may also prove beneficial.

Acknowledgments—We thank Dr. Xiaobo Zhou for expert help in developing NeuriteIQ software. We thank Bradley T. Hyman for support.

REFERENCES

1. Palop, J. J., and Mucke, L. (2010) Amyloid-β-induced neuronal dysfunction in Alzheimer disease: from synapses toward neural networks. *Nat. Neurosci.* **13,** 812–818
2. Knobloch, M., and Mansuy, I. M. (2008) Dendritic spine loss and synaptic alterations in Alzheimer disease. *Mol. Neurobiol.* **37,** 73–82
3. Shankar, G. M., Li, S., Mehta, T. H., Garcia-Munoz, A., Shepardson, N. E., Smith, I., Brett, F. M., Farrell, M. A., Rowan, M. J., Lemere, C. A., Regan, C. M., Walsh, D. M., Sabatini, B. L., and Selkoe, D. J. (2008) Amyloid-β protein dimers isolated directly from Alzheimer's brains impair synaptic plasticity and memory. *Nat. Med.* **14,** 837–842
4. Irizarry, M. C., McNamara, M., Fedorchak, K., Hsiao, K., and Hyman, B. T. (1997) APPSw transgenic mice develop age-related Aβ deposits and neuropil abnormalities, but no neuronal loss in CA1. *J. Neuropathol. Exp. Neurol.* **56,** 965–973
5. Schmidt, E. R., Pasterkamp, R. J., and van den Berg, L. H. (2009) Axon guidance proteins: novel therapeutic targets for ALS? *Progress Neurobiol.* **88,** 286–301
6. Jellinger, K. A. (2009) Formation and development of Lewy pathology: a critical update. *J. Neurol.* **256,** Suppl. 3, 270–279
7. Szekely, C. A., and Zandi, P. P. (2010) Non-steroidal anti-inflammatory drugs and Alzheimer disease: the epidemiological evidence. *CNS Neurological Disorders Drug Targets* **9,** 132–139
8. Zhang, Y., Zhou, X., Degterev, A., Lipinski, M., Adjeroh, D., Yuan, J., and Wong, S. T. (2007) A novel tracing algorithm for high throughput imaging. Screening of neuron-based assays. *J. Neurosci. Methods* **160,** 149–162
9. Huang, Y., Zhou, X., Miao, B., Lipinski, M., Zhang, Y., Li, F., Degterev, A., Yuan, J., Hu, G., and Wong, S. T. (2010) A computational framework for studying neuron morphology from *in vitro* high content neuron-based screening. *J. Neurosci. Methods* **190,** 299–309
10. Loh, S. H., Francescut, L., Lingor, P., Bähr, M., and Nicotera, P. (2008) Identification of new kinase clusters required for neurite outgrowth and retraction by a loss-of-function RNA interference screen. *Cell Death Differ.* **15,** 283–298
11. Cole, G. M., and Frautschy, S. A. (2010) Mechanisms of action of non-steroidal anti-inflammatory drugs for the prevention of Alzheimer dis-

ease. *CNS Neurological Disorders Drug Targets* **9,** 140–148
12. Dargahi, L., Nasiraei-Moghadam, S., Abdi, A., Khalaj, L., Moradi, F., and Ahmadiani, A. (2011) Cyclooxygenase (COX)-1 activity precedes the COX-2 induction in Aβ-induced neuroinflammation. *J. Mol. Neurosci.* **45,** 10–21
13. Jarrett, J. T., Berger, E. P., and Lansbury, P. T., Jr. (1993) The C-terminus of the beta protein is critical in amyloidogenesis. *Ann. N.Y. Acad. Sci.* **695,** 144–148
14. Dill, J., Patel, A. R., Yang, X. L., Bachoo, R., Powell, C. M., and Li, S. (2010) A molecular mechanism for ibuprofen-mediated RhoA inhibition in neurons. *J. Neurosci.* **30,** 963–972
15. Selkoe, D. J. (2002) Deciphering the genesis and fate of amyloid beta-protein yields novel therapies for Alzheimer disease. *J. Clinic. Investig.* **110,** 1375–1381
16. Sperling, R. A., Aisen, P. S., Beckett, L. A., Bennett, D. A., Craft, S., Fagan, A. M., Iwatsubo, T., Jack, C. R., Kaye, J., Montine, T. J., Park, D. C., Reiman, E. M., Rowe, C. C., Siemers, E., Stern, Y., Yaffe, K., Carrillo, M. C., Thies, B., Morrison-Bogorad, M., Wagster, M. V., and Phelps, C. H. (2011) *Alzheimers Dement.* **7,** 280–292
17. Conejero-Goldberg, C. T., and Davies, P. (2008) Effects of cell cycle inhibitors on tau phosphorylation in N2aTau3R cells. *J. Mol. Neurosci.* **35,** 7
18. Brioni, J. D., Garrison, T. R., Bitner, S. R., and Cowart, M. D. (2011) Discovery of histamine H3 antagonists for the treatment of cognitive disorders and Alzheimer's disease. *J. Pharmacol. Exp. Ther.* **336,** 13
19. Lee, Y. J., Han, S. B., Nam, S. Y., Oh, K. W., and Hong, J. T. (2010) Inflammation and Alzheimer disease. *Arch. Pharm. Res.* **33,** 1539–1556
20. Kotilinek, L. A., Westerman, M. A., Wang, Q., Panizzon, K., Lim, G. P., Simonyi, A., Lesne, S., Falinska, A., Younkin, L. H., Younkin, S. G., Rowan, M., Cleary, J., Wallis, R. A., Sun, G. Y., Cole, G., Frautschy, S., Anwyl, R., and Ashe, K. H. (2008) Cyclooxygenase-2 inhibition improves amyloid-β-mediated suppression of memory and synaptic plasticity. *Brain* **131,** 651–664
21. Cakala, M., Malik, A. R., and Strosznajder, J. B. (2007) Inhibitor of cyclooxygenase-2 protects against amyloid β peptide-evoked memory impairment in mice. *Pharmacol. Reports* **59,** 164–172
22. Takeda, T., Kumar, R., Raman, E. P., and Klimov, D. K. (2010) Nonsteroidal anti-inflammatory drug naproxen destabilizes Aβ amyloid fibrils: a molecular dynamics investigation. *J. Phys. Chem. B* **114,** 15394–15402
23. Fu, Q., Hue, J., and Li, S. (2007) Nonsteroidal anti-inflammatory drugs promote axon regeneration via RhoA inhibition. *J Neurosci.* **27,** 4154–4164
24. Weggen, S., Eriksen, J. L., Das, P., Sagi, S. A., Wang, R., Pietrzik, C. U., Findlay, K. A., Smith, T. E., Murphy, M. P., Bulter, T., Kang, D. E., Marquez-Sterling, N., Golde, T. E., and Koo, E. H. (2001) A subset of NSAIDs lower amyloidogenic Aβ42 independently of cyclooxygenase activity. *Nature* **414,** 212–216
25. Vlad, S. C., Miller, D. R., Kowall, N. W., and Felson, D. T. (2008) Protective effects of NSAIDs on the development of Alzheimer disease. *Neurology* **70,** 1672–1677
26. Hayden, K. M., Zandi, P. P., Khachaturian, A. S., Szekely, C. A., Fotuhi, M., Norton, M. C., Tschanz, J. T., Pieper, C. F., Corcoran, C., Lyketsos, C. G., Breitner, J. C., and Welsh-Bohmer, K. A. (2007) Does NSAID use modify cognitive trajectories in the elderly? The Cache County study. *Neurology* **69,** 275–282
27. Szekely, C. A., Breitner, J. C., Fitzpatrick, A. L., Rea, T. D., Psaty, B. M., Kuller, L. H., and Zandi, P. P. (2008) NSAID use and dementia risk in the Cardiovascular Health Study: role of APOE and NSAID type. *Neurology* **70,** 17–24
28. Grodstein, F., Skarupski, K. A., Bienias, J. L., Wilson, R. S., Bennett, D. A., and Evans, D. A. (2008) Anti-inflammatory agents and cognitive decline in a bi-racial population. *Neuroepidemiology* **30,** 45–50
29. Aisen, P. S., Schafer, K. A., Grundman, M., Pfeiffer, E., Sano, M., Davis, K. L., Farlow, M. R., Jin, S., Thomas, R. G., and Thal, L. J. (2003) Effects of rofecoxib or naproxen vs placebo on Alzheimer disease progression: a randomized controlled trial. *JAMA* **289,** 2819–2826
30. Sato, T., Hanyu, H., Hirao, K., Kanetaka, H., Sakurai, H., and Iwamoto, T. (2011) Efficacy of PPAR-γ agonist pioglitazone in mild Alzheimer disease. *Neurobiol. Aging* **32,** 1626–1633